

Low-frequency method for magnetothermopower and Nernst effect measurements on single crystal samples at low temperatures and high magnetic fields

E. S. Choi, J. S. Brooks, J. S. Qualls, and Y. S. Song

Citation: [Review of Scientific Instruments](#) **72**, 2392 (2001); doi: 10.1063/1.1353192

View online: <http://dx.doi.org/10.1063/1.1353192>

View Table of Contents: <http://scitation.aip.org/content/aip/journal/rsi/72/5?ver=pdfcov>

Published by the [AIP Publishing](#)

Articles you may be interested in

[Irreversibility and anisotropy of the low-temperature magnetization in manganites. Spin-glass polyamorphism](#)
Low Temp. Phys. **40**, 179 (2014); 10.1063/1.4865567

[Thin-film alternating current nanocalorimeter for low temperatures and high magnetic fields](#)

Rev. Sci. Instrum. **76**, 043906 (2005); 10.1063/1.1889432

[A newly developed high-pressure cell by using modified Bridgman anvils for precise measurements in magnetic fields at low temperatures](#)

Rev. Sci. Instrum. **73**, 1828 (2002); 10.1063/1.1458044


[Low-frequency ac measurement of the Seebeck coefficient](#)

Rev. Sci. Instrum. **72**, 4201 (2001); 10.1063/1.1406930


[Measurement of the thermoelectric power of very small samples at ambient and high pressures](#)

Rev. Sci. Instrum. **70**, 3586 (1999); 10.1063/1.1149964


Frustrated by old technology?



Is your AFM dead and can't be repaired?



Sick of bad customer support?




It is time to upgrade your AFM

Minimum \$20,000 trade-in discount for purchases before August 31st

Asylum Research is today's technology leader in AFM

dropmyoldAFM@oxinst.com



The Business of Science®

Low-frequency method for magnetothermopower and Nernst effect measurements on single crystal samples at low temperatures and high magnetic fields

E. S. Choi

*Department of Physics, Ewha Womans University, Seoul 120-750, Korea
and National High Magnetic Field Laboratory, Florida State University, Tallahassee, Florida 32310*

J. S. Brooks^{a)} and J. S. Qualls^{b)}

*National High Magnetic Field Laboratory and Physics Department, Florida State University,
Tallahassee, Florida 32310*

Y. S. Song

Texas Center for Superconductivity, University of Houston, Houston, Texas 77204-5932

(Received 19 September 2000; accepted for publication 11 January 2001)

We describe an alternating current method for the measurement of the longitudinal (S_{xx}) and transverse (S_{xy} , i.e., Nernst) thermopower of millimeter-size crystal samples at low temperatures ($T < 1$ K) and high magnetic fields ($B \sim 30$ T). A low-frequency (33 mHz) heating method is used to increase the resolution and to determine the temperature gradient reliably in high magnetic fields. Samples are mounted between two thermal blocks which are heated by a sinusoidal frequency f_0 with a $\pi/2$ phase difference. The phase difference between two heater currents gives a temperature gradient at $2f_0$. The corresponding thermopower and Nernst effect signals are extracted by using a digital signal processing method due to the low frequency of the measurement. An important component of the method involves a superconducting link, $\text{YBa}_2\text{Cu}_3\text{O}_{7+\delta}$, which is mounted in parallel with sample to remove the background magnetothermopower of the lead wires. The method is demonstrated for the quasi-two-dimensional organic conductor $\alpha\text{-(BEDT-TTF)}_2\text{KHg(SCN)}_4$, which exhibits a complex, magnetic field dependent ground state above 22.5 T at low temperatures.

© 2001 American Institute of Physics. [DOI: 10.1063/1.1353192]

I. INTRODUCTION

The application of a thermal gradient (ΔT) across a conducting material leads to a corresponding potential difference, or thermoelectric power [(TEP) or thermopower]. Thermopower measurements yield information about both thermodynamic properties and the transport properties of carriers. Advantages of TEP include the zero-current nature of the measurement, and its sensitivity to band structure, especially in the case of anisotropic (low dimensional Fermi surface) materials. Following Mott and Jones, the thermopower¹ of a metal may be expressed as

$$S = \frac{\pi^2 k_B^2 T}{3e} \left(\frac{d \ln n(E)}{dE} + \frac{d \ln v^2(E)}{dE} + \frac{d \ln \tau(E)}{dE} \right)_{E=E_F}, \quad (1)$$

where $n(E)$ is the density of the states, $v(E)$ is an average charge velocity, and $\tau(E)$ is the carrier scattering relaxation time. As we will show in the present application, the derivative of $n(E)$ at the Fermi energy will lead to large oscillations in systems where Landau quantization of the electronic

energy levels occurs at high magnetic fields.² Hence, oscillations in TEP associated with the de Haas van-Alphen effect can be observed.

In a typical experimental setup, similar to that shown in Fig. 1, a sample is connected between two thermal platforms. A temperature difference is applied by heating one of the platforms, and ΔT is measured either between the platforms, or at points on the sample. The electric potential difference ΔV is measured with contact leads on the sample. In general, the apparatus is in weak thermal contact with a reference bath at a variable temperature T . As with other such measurements on small samples (e.g., specific heat), the effects of the addenda, and the magnetic field dependence of the sensors, cannot be neglected. Previous magnetothermopower (MTEP) measurements at low temperatures and in high magnetic fields have addressed experimental issues such as the magnetothermopower of lead wires.^{3,4} By using well-studied elemental metal wires of copper or gold, and high T_c superconductors (where $S=0$ for $T \ll T_c$ and $B \ll B_{c2}$), these background contributions may be sorted out. For long, thin samples (millimeter-size-samples with 10:1–100:1 aspect ratios), and alternating current (ac) technique has been used to measure MTEP for a wide range of temperature.⁵ But these techniques cannot be easily adapted to small single crystals with 1:1 aspect ratios, as in the case of the quasi-two-dimensional “ET” organic conductors (see Sec. III), where an accurate determination of ΔT in high magnetic fields be-

^{a)}Author to whom correspondence should be addressed; electronic mail: brooks@magnet.fsu.edu

^{b)}Present address: Physics Dept., Wake Forest University, Winston-Salem, NC 27109.

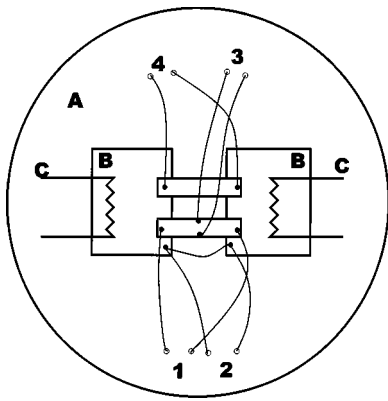


FIG. 1. Diagram of the measurement holder (the outer diameter of the cylindrical copper holder is 10 mm). A: Cu heat sink, B: quartz blocks, and C: heaters. 1: thermopower leads of sample, 2: Chromel–Au(Fe0.07%) thermocouples for ΔT leads, 3: Nernst voltage leads of sample, and 4: thermopower leads of reference YBCO sample.

comes difficult. Resel *et al.* introduced a MTEP measurement technique up to 17 T and down to 3 K where chromel-constantan thermocouples are used as voltage and ΔT leads simultaneously.⁶ Their technique (as does ours) includes the alternate heating method (“seesaw heating”) to increase the measurement accuracy. However, there are limits in their methods in the case of small samples, since the large absolute TEP of chromel wire can introduce substantial background signal, and the application of a thermocouple junction directly to a small sample, can cause complications.

The technique to be introduced in this article utilizes a stable, alternating heating method at very low frequency. Here the lead wires are *in situ* calibrated using a $\text{YBa}_2\text{Cu}_3\text{O}_{7+\delta}$ high T_c superconductor sample as a reference. When combined with digital signal processing methods, our procedure leads to enhanced resolution and accuracy for the MTEP of small samples, with direct application to high magnetic field measurements.

II. EXPERIMENTAL TECHNIQUE

A. Measurement setup

Figure 1 shows the schematic diagram of the MTEP and the Nernst effect measurement holder in a top view, where the magnetic field is applied normal to the plane of the figures. The apparatus is held in a 10 mm diameter cylindrical copper holder that is sealed with a copper cap (with a threaded grease seal). The copper holder can be maintained at any temperature T between 300 and 0.5 K in a standard cryogenic, high-field dewar arrangement. The integrity of the seal is checked by a small jump in an applied temperature gradient of the apparatus when the encapsulated air in the holder condenses out below 80 K. Since ^3He exchange gas is used to cool the holder, superfluid leaks to not present a problem. Samples are mounted between two quartz blocks ($2.9 \times 2.4 \times 1.0 \text{ mm}^3$), A and B, with the ends attached using Apiezon N grease.⁷ Electrical contacts to the samples are made by $12.5 \mu\text{m}$ gold wires using silver (or carbon) paste. The electrical connection between the lead wires and the external wires is kept in an isothermal condition by thermally anchoring them to the copper holder. Chromel–

Au(Fe0.07%) thermocouple wires,⁷ used to measure ΔT between the quartz blocks, are attached to the quartz blocks using Stycast 2850 GT epoxy.⁸ To minimize the experimental inaccuracy, which may result from the difference of temperature between the quartz block and the sample, the temperature gradient was produced by heating quartz blocks at a low frequency of order 33 mHz. Two chip resistor heaters (220Ω RuO_2 miniature surface-mount resistors) are attached by Stycast 2850 GT epoxy⁸ to the edge of quartz blocks to enhance the homogeneous heat conduction.

Two sinusoidal currents are applied by Keithley 220 programmable direct current (dc) current sources⁹ with same frequency f_0 but with a $\pi/2$ phase difference. The relation between the two heater currents and ΔT for ideal system (perfect heat conduction from the heater to the quartz block) is the following:

$$I_1(t) = I_0 \sin(2\pi f_0 t),$$

$$I_2(t) = I_0 \sin(2\pi f_0 t + \pi/2) = I_0 \cos(2\pi f_0 t), \quad (2)$$

$$\Delta T(t) \propto (I_1^2 - I_2^2)R/C_p = -I_0^2 R/C_p \cos[2\pi(2f_0)t],$$

where I_1 and I_2 are heater currents, R is heater resistance, C_p is the heat capacity of the quartz block, and t is the time. The validity of last expression in Eq. (2), i.e., the assumption of equal power for both heaters, can be checked by the Fourier analysis of the voltage signal of thermocouple wires. If the values of R and C_p are not identical, components other than the second harmonic ($f = 2f_0$) can appear in the Fourier spectrum. For apparatus described here, the component parameters were very well matched, and the first harmonic ($f = f_0$) contributed only about 2% to the total signal. Hence, for our purpose, we considered only the dominant $2f_0$ contribution in our analysis. Since ΔT oscillates with $2f_0$ frequency, corresponding TEP and the Nernst voltage will also oscillate with the same frequency. This second harmonic detection has an advantage in reducing electrical crosstalk which may arise from single harmonic generation in the heaters.

Figures 2(a) and 2(b) show the applied heater currents and the corresponding thermoelectric potential ΔV_1 and the thermocouple electromotive force (emf) ΔV_2 as a function of the time. (ΔV_1 and ΔV_2 refer to voltage leads 1 and 2 as shown in Fig. 1) ΔV_2 , the measured emf of the Chromel–Au(Fe0.07%) thermocouple, is related to ΔT by $\Delta V_2 = -\Delta T S_{\text{Ch-AuFe}} + V_{\text{offset}}$, where $S_{\text{Ch-AuFe}}$ is the TEP of Chromel–Au(Fe0.07%) thermocouples⁷ and V_{offset} is the offset voltage which lies in the range of 0.1 – $0.2 \mu\text{V}$ at low temperature. ΔV_1 and ΔV_2 were measured with Keithley 2182 nanovoltmeters.⁹ There is a slight phase difference ($\sim 14^\circ$ or about 0.6 s delay between ΔT and ΔV_2 due to the nonideal heat conduction. However, since the signals are digitally averaged over $2\frac{1}{2}$ periods (see later) to obtain the amplitudes of ΔT and ΔV_2 , the phase difference does not enter into the final TEP value. Also, because the method involves the peak-to-peak (pp) values of ΔT and ΔV_2 , V_{offset} will not enter the final value of ΔT_{pp} used to find the thermopower. When ΔT_{pp} is small compared to the measurement temperature T , the absolute TEP (S_{xx}) and Nernst voltage (S_{xy}) can be expressed as

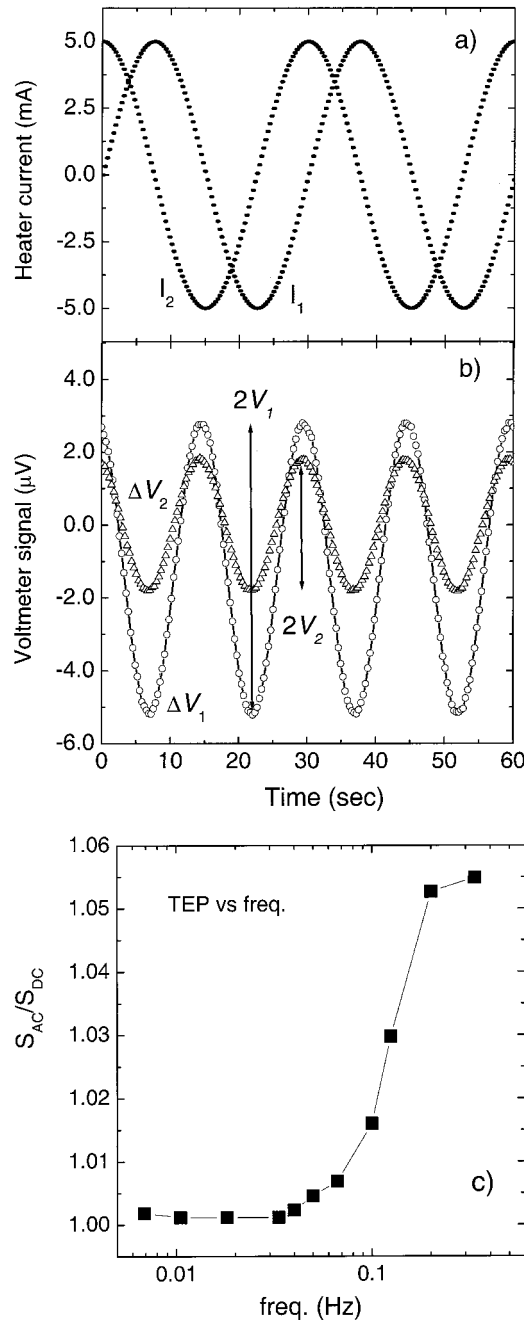


FIG. 2. (a) Heater currents and (b) ΔV_1 (ΔV_2) as a function of the time. The period of the heating cycle is 30 s and the corresponding periods of oscillation of temperature gradient and thermopower signal are 15 s. (c) S_{ac}/S_{dc} vs frequency method used to determine the optimum frequency range where $S_{ac}/S_{dc} \approx 1$ for the TEP measurements.

$$\begin{aligned}
 S_{xx}(T, B) &= \frac{V_1(T, B)}{\Delta T(T, B)_{pp}} P_{xx}(T, B) + S_{Au}(T, B) \\
 &= \frac{V_1(T, B)}{V_2(T, B)/S_{Ch-AuFe}(T, B)} P_{xx}(T, B) \\
 &\quad + S_{Au}(T, B), \\
 S_{xy}(T, B) &= \frac{V_3(T, B)}{V_2(T, B)/S_{Ch-AuFe}(T, B)} P_{xy}(T, B),
 \end{aligned} \tag{3}$$

where S_{Au} is the absolute thermopower of Au and P is either

+1 or -1 depending on the phase difference between V_1 (V_3) and V_2 . S_{Au} can be determined from the measurement of another sample [YBa₂Cu₃O_{7+δ} (YBCO) in this article] whose value is known at a certain temperature and magnetic field. For the Nernst voltage, it is assumed that sample alignment is ideal so that there is no contribution from S_{xx} . When the misalignment is substantial, S_{xy} can be obtained from the difference in the Nernst voltage for two magnetic field sweeps with opposite polarities.

The amplitude of oscillation (V_1 and V_2 in Fig. 2) can be determined from the discrete values (ΔV_i) by the following formula:¹⁰

$$V = \sqrt{\sigma_x^2 [H\{\Delta V_i - 2\mu_x[H(\Delta V_j)]\}] / (8/3\sqrt{2})}, \tag{4a}$$

where σ_x^2 is the variance, μ_x is the mean value, and $H(x_i)$ is the Hanning window defined by

$$\begin{aligned}
 H(x_i) &= 0.5 \left[1 - \cos\left(\frac{2\pi i}{\text{\# of elements}}\right) \right] \\
 &\text{for } i = 0, 1, 2, \dots, n-1.
 \end{aligned} \tag{4b}$$

The Hanning window was used to separate ac signal from dc signal (V_{offset}), and hence, the signal was compensated for the windowing effect by a multiplicative constant (8/3 in this case). Finally, the root mean square value was used to extract an amplitude of the ac signal. Because this method does not discriminate oscillations with different frequencies (for example, dominate $2f_0$ signal and f_0 signal from nonidentical heat transfer), this method has an advantage that the non-identical heat transfer term can be also considered. However, if there is a substantial low frequency noise, one should use digital bandpass filter or fast Fourier transform analysis to obtain the amplitudes.

The advantage of the ac method is that phase sensitive detection of the signal can be employed, thereby improving the signal-to-noise factors in high-field, water-cooled, resistive magnets where there is inevitably vibration and field fluctuations. We note that there have been previous ac TEP measurements using the $2f_0$ mode by Kettler *et al.*,¹¹ where limitations due to the heat capacity of the material and the characteristic times of thermal relaxation were identified. To overcome these problems, the excitation frequency $2f_0$ should be as small as possible. In our measurement setup, $2f_0$ was chosen to be 67 mHz, i.e., the oscillation period of the heater currents is 30 s, and the corresponding oscillation period of ΔT is 15 s. Our method for determining the frequency range where the ac and ideal dc methods coincide is shown in Fig. 2(c). A suitable excitation frequency range for the apparatus in Fig. 1 is for $2f_0$ below 100 mHz. Above 100 mHz, the ac TEP increases as a function of frequency due to various thermal relaxation rates which are characteristic of the apparatus.

B. Measurements in magnetic field

The difficulties for the MTEP measurement comes from the field dependence of $S_{Au}(B)$ and $S_{Ch-AuFe}(B)$. To avoid the problem of $S_{Ch-AuFe}(B)$, we exploit the high reproducibility of ΔT for corresponding constant amplitudes of the heater currents. V_2 changes very little with time during a

measurement for fixed temperature (typically less than 1 mK over a 20 min period of measurement). Correspondingly, the change of ΔT is also very small for magnetic field sweeps, with less than 1% deviation in ΔT as compared with the zero field value. The change of ΔT will come from the field dependence of specific heat of the quartz block and the magnetoresistance of the heater resistor. The former is negligible for the quartz block and the latter can be calibrated at each magnetic field. Although the magnetoresistance [MR = $R(B)/R(B=0)$] of the chip resistor used in this measurement is very small (for 30 T: $\sim -1.5\%$ at 4 K, $\sim -1.4\%$ at 1.1 K, $\sim -2.0\%$ at 0.7 K), we also included the MR effect in the determination of $\Delta T(T, B)$. Once $\Delta T(T, B)$ is determined, $S_{\text{Au}}(B)$ can be easily measured using a YBCO sample as a reference below its critical field, where $S_{\text{YBCO}}(B) = 0$. Therefore the MTEP and Nernst voltage can be written as

$$S_{xx}(T, B) = \frac{V_1(T, B)}{\frac{V_2(T, B=0)}{S_{\text{Ch-AuFe}}(T, B=0)} \text{MR}(T, B)} P_{xx}(T, B) + S_{\text{Au}}(T, B),$$

$$S_{xy}(T, B) = \frac{V_3(T, B)}{\frac{V_2(T, B=0)}{S_{\text{Ch-AuFe}}(T, B=0)} \text{MR}(T, B)} P_{xy}(T, B),$$

where

$$S_{\text{Au}}(T, B) = 0 - \frac{V_1(T, B)}{\frac{V_2(T, B=0)}{S_{\text{Ch-AuFe}}(T, B=0)} \text{MR}(T, B)} P_{xx-\text{YBCO}}(T, B)$$

for $T < T_c$ and $B < B_c$ of YBCO. (6)

III. EXPERIMENTAL RESULTS

To demonstrate the techniques described here, we consider the MTEP and the Nernst effect of organic conductor $\alpha\text{-(BEDT-TTF)}_2\text{KHg(SCN)}_4$. The material $\alpha\text{-(BEDT-TTF)}_2\text{KHg(SCN)}_4$ is a well known quasi-two-dimensional organic conductor¹² which shows metal-density wave transition around $T = 8$ K, and which has a magnetoresistance anomaly at 22.5 T (below 8 K) where there is a magnetic field induced change in the electronic structure. The typical size of the sample is about $1.4 \times 0.6 \times 0.26$ mm³, with a plate-like morphology. The sample is mounted so that the temperature gradient is in the plane of the conducting layers (a or c axis), with the field perpendicular to the conducting layers (b axis). A polycrystalline YBCO sample, of comparable dimensions, was used for *in situ* calibration. The sample holder was attached to the probe of ³He cryostat and a 30 T resistive magnet at the National High Magnetic Field Laboratory was used for the high field measurements.

Figure 3 shows zero field TEP results of the crystallographic a and c axis, i.e., ΔT is parallel with a and c axis, respectively. As mentioned in the Introduction, the TEP is sensitive to the anisotropy of the band structure (and therefore the Fermi surface), hence, it depends on the direction of ΔT with respect to the crystallographic axes. Structure in the

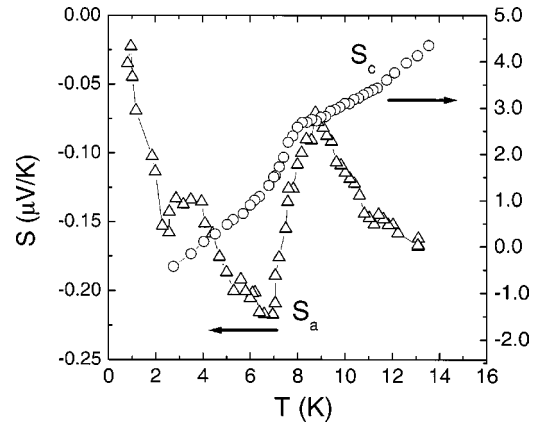


FIG. 3. Zero-field thermopower results of $\alpha\text{-(BEDT-TTF)}_2\text{KHg(SCN)}_4$ as a function of temperature. A gap opens in the quasi-one-dimensional part of the Fermi surface near 8 K, which is seen as a peak in the a -axis data. Open triangles: $\Delta T \parallel a$ axis, open circles: $\Delta T \parallel c$ axis.

TEP, due to the opening of a partial gap, is clearly seen around 8 K for both axes. This behavior is the result of two bands, i.e., both open and closed orbits (with conductivities σ_0 and σ_c) in the a - c plane that contribute to the total thermopower (S), as weighted by the electrical conductivities as $S_{\text{total}} = S_0 * \sigma_0 / (\sigma_0 + \sigma_c) + S_c * \sigma_c / (\sigma_c + \sigma_0)$. Above $T = 8$ K, both orbits have metallic conductivity; hence, the total thermopower shows a linear temperature dependence. Below $T = 8$ K, a band gap opens for open orbit band, σ_0 goes to zero exponentially, and S_0 diverges as $1/T$. However, below this temperature a modified closed orbit band remains, which still gives a metallic thermopower contribution. Just below the transition temperature there will be a jump of thermopower from the divergence of S_0 , but this contribution quickly disappears as σ_0 goes to zero. The sum of the three contributions (from the three different axes) to the jump is about 1 $\mu\text{V/K}$, which is in reasonable agreement with heat capacity measurements.¹³

For MTEP and the Nernst effect measurement, the magnetic field is swept very slowly (0.042 T/min) for fixed temperatures. Figure 4(a) shows the raw data of ΔV_1 , ΔV_2 , and ΔV_3 for $T = 0.7$ K. When the heater power is about 220 μW , ΔT is 0.085 K at zero field and it is assumed to decrease to 0.083 K at $B = 27$ T due to the negative MR of the chip resistor. The oscillation of V_1 and V_3 is huge and the change of polarity [$P(T, B)$ of Eqs. (3) and (5)] can be also seen from the raw data. The derived MTEP data are shown in Fig. 4(b). Each MTEP data point is obtained using Eqs. (4)–(6) by averaging over ~ 100 raw data points.

Figure 5 shows the Nernst voltage (S_{xy}) for positive and negative magnetic field sweep and the corresponding Nernst effect at $T = 1.4$ K. For this case, the xy sample electrode alignment is quite good and quantum oscillations can be clearly seen, even though the final result are obtained by subtracting $S_{xy}(B < 0)$ from $S_{xy}(B > 0)$, and dividing by 2. The corresponding period of quantum oscillations can be obtained from the Fourier transform, and it is found to be ~ 670 T, which agrees with the value measured from the magnetoresistance and magnetization experiments.¹⁴

Finally, we describe the MTEP of the thermocouple

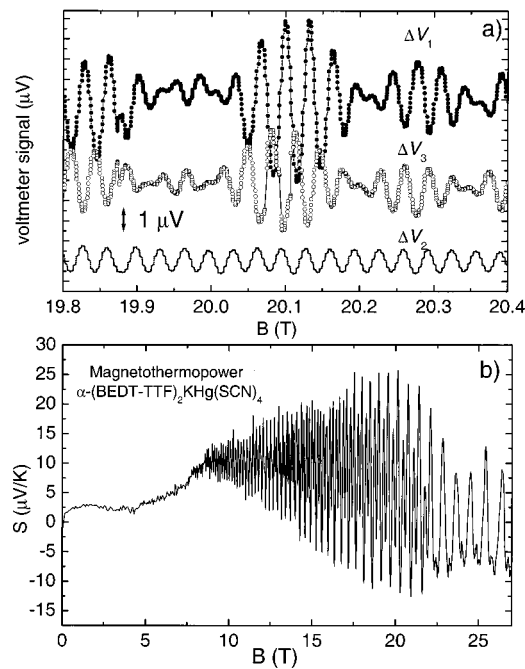


FIG. 4. Magnetothermopower. (a) ΔV_1 , ΔV_2 , and ΔV_3 curves under magnetic field for α -(BEDT-TTF) $_2$ KHg(SCN) $_4$ at $T=0.7$ K. (b) Derived magnetothermopower results. Note the narrow range of field in (a), which corresponds to only a few quantum oscillations in (b).

(Chromel–AuFe) and electrical (Au) leads used in the present study. This is done under the assumption that ΔT depends only on the heater power (taking into account the negative MR), and assuming that the magnetic field effect on the heat capacity of quartz and Stycast epoxy is negligible. Then, for a fixed heater power (ΔT) and temperature T , ΔV_4

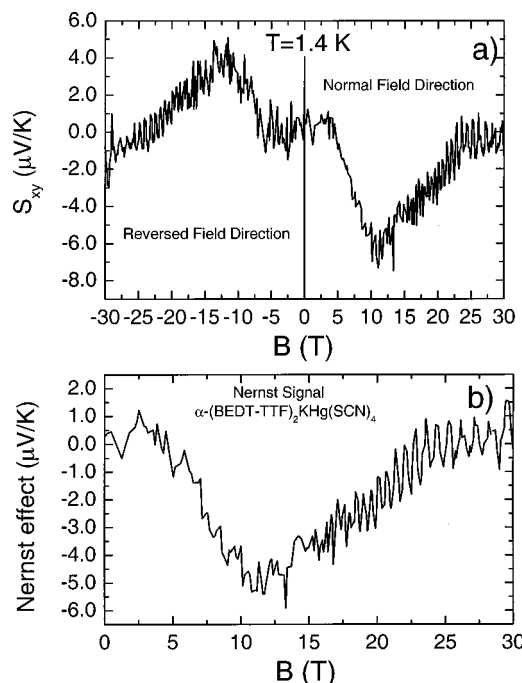


FIG. 5. Nernst effect. (a) S_{xy} signal of α -(BEDT-TTF) $_2$ KHg(SCN) $_4$ for normal and reversed field sweeps at $T=1.4$ K. The large asymmetry, even in the raw data, indicates a significant xy component of the thermopower. (b) Corresponding Nernst voltage $\{[S_{xy}(B>0)-S_{xy}(B<0)]/2\}$.

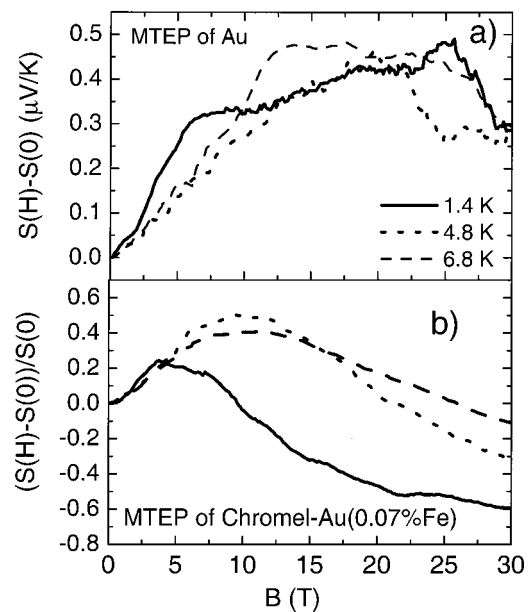


FIG. 6. (a) $[S(B)-S(B=0)]$ of Au and (b) $[S(B)-S(B=0)]/S(B=0)$ of Chromel–Au(Fe0.07%) thermocouples.

on the YBCO sample and ΔV_2 on the quartz blocks are measured as a function of magnetic field. $S_{\text{Au}}(T, B)$ can then be determined directly, and from Eq. (6), we can determine $S_{\text{Ch–AuFe}}(T, B)$. Figure 6 shows the results at different temperatures as a function of the magnetic field. For the MTEP of $S_{\text{Ch–AuFe}}$, the overall behavior is quite similar to the previous determinations¹⁵ in which the MTEP was measured by a different method up to $B=14$ T.

ACKNOWLEDGMENTS

This work was supported in part by NSF-DMR95-10427 and DMR99-71474. The work was carried out at the National High Magnetic Field Laboratory, Supported by a contractual agreement between the State of Florida and the NSF through NSF-DMR-95-27035. E. S. Choi was financially supported by the KOSEF postdoctoral fellowship program.

- ¹See N. F. Mott and H. Jones, in D. K. C. MacDonald, *Thermoelectricity: An Introduction to the Principles* (Wiley, New York, 1962), p. 56.
- ²F. J. Blatt, P. A. Schroeder, and C. L. Folies, *Thermoelectric Power of Metals* (Plenum, New York, 1976).
- ³W. Kang, S. T. Hannahs, L. Y. Ching, R. Upasani, and P. M. Chaikin, *Phys. Rev. B* **45**, 13566 (1992).
- ⁴H.-C. Ri, R. Gross, F. Gollnik, A. Beck, R. P. Huebener, P. Wagner, and H. Adrian, *Phys. Rev. B* **50**, 3312 (1994).
- ⁵W. H. Kettler, R. Wernhardt, and M. Rosenberg, *Rev. Sci. Instrum.* **57**, 3053 (1986).
- ⁶R. Resel, E. Gratz, A. T. Burkov, T. Nakama, M. Higa, and K. Yagasaki, *Rev. Sci. Instrum.* **67**, 1970 (1996).
- ⁷The Apiezon N Grease and Chromel–Au(Fe0.07%) thermocouple wires (0.127 mm diameter) were purchased from LakeShore Cryotronics, Inc., 575 McCorkle Blvd., Westerville, OH 43082.
- ⁸Emerson and Cuming, 46 Mannign Road, Billerica, MA 01821.
- ⁹Keithley Instruments, Inc., 28775 Aurora Road, Cleveland, OH 44139.
- ¹⁰*Labview Analysis VI Reference Manual*, The National Instruments Co. (1998), National Instruments Corporation 11500 N. Mopac Expwy., Austin, TX 78759-3504.

- ¹¹See Kettler *et al.*, in L. L. Sparks and R. L. Powell, *Temperature, Its Measurement and Control in Science and Industry* (Instrument Society of America, Pittsburgh, 1972), Vol. IV, Pt. 3, p. 1569.
- ¹²T. Ishiguro, G. Saito, and K. Yamaji, *Organic Superconductors*, 2nd ed. (Springer, Berlin, 1998).
- ¹³A. Kovalev, H. Mueller, and M. V. Kartsovnik, JETP **86**, 578 (1998).
- ¹⁴J. Wosnitza, *Fermi Surfaces of Low-Dimensional Organic Metals and Superconductors* (Springer, Berlin, 1996).
- ¹⁵H. H. Sample, L. J. Neuringer, and L. G. Rubin, Rev. Sci. Instrum. **45**, 64 (1974).